A SEARCH FOR SHORT PERIOD VARIABLE STARS

COURTNEY FAGG

UNDERGRADUATE THESIS

SOUTHERN METHODIST UNIVERSITY

DEPARTMENT OF PHYSICS

Dallas, TX 75275

Abstract

I present a search for stars that demonstrate rapidly changing visible light curves. The data that I have used for this search has been procured from the ROTSE1 telescope's archival data of the night of April 14, 2000. This field covers eight degrees of the night sky, and was observed for approximately six continuous hours in one night. By using general statistical properties of the light curves, I was able to narrow my search to obtain clearly varying light curves. The analysis has shown to be most effective for light curve variations with periods < 0.3 days that possess magnitude variations greater than 0.1, and mean magnitude values varying in the range of 10 to 15. My search has produced 20 variable star candidates, whose classification will be based solely on their light curve characteristics. I have observed phenomena such as δ Scuti and W UMa stars in my data collection. The presence of these short period variable stars proves the effectiveness of our method of searching.

Table of Contents

List of Tables

List of Figures

I. Introduction

Stars with varying magnitudes (known as variable stars) have interested astronomers for hundreds of years, beginning with the first supernovae with pulsating light variations that were observed and documented. Since then, thousands of variable stars have been discovered and classified based on their peculiarities in variation. The observation of these interstellar phenomena have allowed astronomers, both amateur and professional, to learn more about the night sky, as well as the night sky not visible to the unaided eye.

Variable stars are grouped into two major categories: intrinsic, whose stars' luminosity varies by pulsating and/or shrinking in size due to physical characteristics, and extrinsic, whose stars appear to vary in magnitude due to an eclipsing companion. An object's magnitude is its dimensionless logarithmic measure of brightness, with lower values corresponding to visually brighter objects. Long period variable stars have been studied for many years because of their apparent brightness changes that can be observed using a telescope, depending on the magnitudes of variation. These stars' period of variation, T, can last from weeks up to several years.

Of increased interest recently have been the short period variable stars, whose T can last from less than an hour to a few days. These types of variables are more commonly observed today because of their high-energy outputs and unusual light curves. Two examples of these types of variables are the RR Lyraes ($0.2 \text{ day} \leq T \leq 1.0 \text{ day}$) and δ Scutis ($T > 0.3$ day), which are *radial pulsators*. The internal inbalance between gravitational and thermal forces causes radial fluctuation in these stars. Once the thermal energy has been temporarily exhausted, the gravitational force causes the star to contract, or appear to "shrink" in size and magnitude, until the internal pressure causes the thermal energy to overcome the gravitational force and expand in size and magnitude. This continuous "pulsing" cycle is shown by a steady oscillating variation in magnitude, and gives this type of variable its name.

Radially pulsating stars are generally divided into two main groups: Cepheid and Cepheid-like stars, and long period variables. The stars identified in this report are Cepheid and Cepheid-like, whose periods are shorter than a day and luminosity cycles are regular. These variables are interesting because their periods of variation indicate their absolute brightness, and therefore their distance. Long period variables are usually red giants whose periods can last up to a year and luminosity cycles are irregular. This type of variable is difficult for the ROTSE telescopes to detect with the data used in this paper, and is therefore disregarded for the purpose of this report.

The apparent magnitude is the "brightness" of the body that is observed from Earth in contrast to the absolute magnitude, which is an intrinsic characteristic of the body derived from the apparent magnitude that is corrected from its distance to its observer. Many telescopes, including those that had recorded the information for this experiment, only measure the apparent magnitude and record it as raw data. Thus, the "magnitudes" of the short period variables discussed in this report are their apparent magnitudes as observed from Earth. The following equation shows the relationship between absolute magnitude (M) and apparent magnitude (m):

$$M = m - 5[(\log_{10} D_L) - 1] \quad \textbf{(1)}$$

where D_L designates the star's luminosity distance in parsecs, where one parsec ≈ 3.2616 light-years.

The discovery of Cepheid variables in the Andromeda Galaxy settled the Island Universe Debate, regarding whether the Milky Way Galaxy was synonymous with the Universe, or simply one within a myriad of other galaxies in the Universe. Cepheid variables observe regular cycles, so their light curve patterns don't appear to change, even from long distances (when it may be expected to see a drop in apparent magnitude, distorting the light curve). Because of this ability to calibrate the distance of the Cepheids in relation to their neighboring stars, astronomers have used Cepheid variables as "standard candles" to determine the speed of their host galaxies that appear to be receding from Earth. These calculations have helped to formulate what is now known as Hubble's Law, which states that the velocity of the galaxies' recession is proportional to their distance from us.

Eclipsing binary systems also exhibit short period behavior, and their light curves are generally characterized by a span of higher magnitude with two small dips of lower magnitude. Binary systems of the W UMa type contain stars that are presumably so close that their surfaces are in contact with one another [1]. The second law of thermodynamics states that the entropy of an isolated system, which is not in equilibrium, will increase until equilibrium is attained. By nature, heat transfers from the body of higher temperature to the body of lower temperature, therefore heat, and thus, luminosity, is transferred from the more massive and hotter star to the less massive and cooler one until both stars acquire equal temperatures. According to this law, it would be expected to see a light curve that is similar to binary systems containing separated stars, though with time, the dips in apparent magnitude would become similar in size, corresponding to the equalization of the stars' temperature and luminosity. However, binary systems with stars whose surfaces do not touch, such as Algol systems, do not experience this transfer of heat and mass, and therefore should exhibit light curves like the general eclipsing type [2].

The Robotic Optical Transient Search Experiment telescope (ROTSE1) is specially designed to observe these short period variables, and has provided the data used in this report. Today, two phases of ROTSE telescopes have been utilized: ROTSE1 and ROTSE3. The telescopes were originally created to study the optical light emitted by gamma ray bursts (GRB) in deep space, but now they are used to study optical light from numerous types of sources, including variable stars. These small but powerful telescopes are distributed around the world for international use [3].

This report explores the results of several searches for variable stars based on different statistical cuts to see which cut values resulted in the largest number of good, clean curves with minimal error. The telescope used to collect the data for this report, ROTSE1 camera 'b', has a position resolution ~ 2 arc seconds [4].

II. Detector and Data

The ROTSE telescopes generate images taken when photons emanating from a light source are focused to an image on an array of cells that send an electric signal based on the intensity of the source. Charged Coupled Devices, or CCDs, are used in many digital photography devices, like digital cameras and ROTSE telescopes. They are responsible for sending the electric signals to be converted to images.

Star images are usually only a pixel wide; however, those for bright stars can be spilled over to multiple cells, creating an excessively bright and distorted image. Many different signals can be obtained over the span of one night. The Interactive Data Language (IDL) computing language was used to compile the signals into a light curve based on magnitude of light intensity versus time, and give an arbitrary number used to identify each object.

III. Selection

The data stored in the University of Michigan's archive can be studied through a special light curve search called "*find_burst*." Data is classified according to search "cuts" that the user inputs, which are based on statistical properties of the light curve. The statistical properties used in this search are variation in magnitude, Δm, the significance of the maximum variation σ_{max}, and χ^2 with respect to a constant brightness.

The cuts used to find the variables determine which curves are "good" or "bad." This means that the light curves that correspond to the selected cuts have clearly varying magnitudes, i.e. they vary by more than the level of error. Most light curves do not vary at all. Some have data with sketchy information (not enough to determine how the light curve is behaving). Through trial and error, sources with clearly varying light curves can be found using specific cuts.

The most obvious sign of a varying light source is the varying magnitude. The change in magnitude, or Δm, is defined as

$$\Delta m = m_{\max} - m_{\min} \tag{2}$$

where m_{max} and m_{min} represent the maximum and minimum magnitudes, respectively. Some light curves exhibit high levels of error that make it difficult to determine whether or not the magnitudes are truly varying. Therefore the observation of a light curve's Δm is not a reliable method on its own, and other cuts are needed to provide supplemental information to detect a light curve with an apparent variation.

The levels of error may differ among the sets of data, depending on factors such as cell overexposure, cloud cover, mechanical vibrations, or most importantly, dim sources of light that ionize fewer atoms in CCD cells. The brightness of these sources cannot be measured well using CCDs since their level of sensitivity cannot fully detect the sources' magnitudes, and can produce higher levels of error. With higher levels of error, it may be difficult to determine how a light source may be varying, if it varies at all. Calculating this level of variation compared to its uncertainty, or its σ_{max}, can help identify a clearer and more precisely varying light curve. It can be found as

$$\sigma_{\max} = \frac{\Delta m}{\sqrt{\varepsilon_{\max}^2 + \varepsilon_{\min}^2}} \tag{3}$$

The "goodness of fit" of an experimental curve based the hypothesis of no variation is best described by its χ^2 distribution. Values of $\chi^2 \sim 1$ are ideal, for this would be the case that the hypothesis agrees with the light curve, given the errors. It is calculated as

$$\chi^2 = \sum_{i=1}^{\infty} \left(\frac{m_i - m_{avg}}{\varepsilon_i} \right)^2 \tag{4}$$

This quantity is calculated by omitting the single observation that is farthest from the m_{avg}, since single anomalous observations are fairly common.

These cuts indicate the level of uncertainty present in each light curve, and smaller levels of error showed clearer curves. However, data as the result of three clear cases of detector problems may also appear. "Saturated" data show very small magnitudes (very bright sources) and may overwhelm the detector. Data that is too "dim" show very large magnitudes, and is usually dominated by electrical "noise" from the detector or atmospheric sources. Data that shows very sparse measurements with no clear indication as to whether or not the source is varying (or if the source is even a light source at all) is called "bad" data. These might occur at the edge of the field or very close to another object. Table 1 below shows the number of stars with saturated, dim, and bad data (N_{sat}, N_{dim}, N_{bad}, respectively) corresponding to each cut value. The last column shows the number of stars exhibiting clearly varying light curves, or "good" data (N_{good}).

Δm	σ_{max}	χ^2	N_{sat}	N_{dim}	N_{bad}	N_{good}
0.5	2.0	3.0	16	41	84	2
0.1	0.0	3.0	28	175	71	11
0.1	0.0	5.0	20	15	11	5
0.5	0.0	3.0	60	117	116	2
0.1	5.0	1.0	59	248	392	16
1.0	2.0	5.0	4	5	5	0
1.0	5.0	0.0	28	23	12	0

TABLE 1 *– Cuts in* find_burst *used in initial image search.*

The images shown in Figures 1-5, along with the data displayed in Table 2 display the light curve data from the best-yielding cuts, including the second cut: $\Delta m = 0.1$, $\sigma_{max} = 0.0$, and $\chi^2 = 3.0$, and fifth cut: $\Delta m = 0.1$, $\sigma_{max} = 5.0$, and $\chi^2 = 1.0$. The remaining cuts yielded a couple of these good light curves, however the majority of the light curves exhibited characteristics that have high levels of error, are incomplete, and/or unclear.

Cuts using $\Delta m = 0.1$ yielded the most light curves. For example, the fifth cut, $\Delta m = 0.1$, $\sigma_{max} = 5.0$, $\chi^2 = 1.0$, yielded 715 light curves. The remaining cuts produced low numbers of N_{good}'s and were not used. Based on these results, it was determined that using $\Delta m = 0.1$ and $\sigma_{max} = 5.0$ would yield the largest number of useful varying light curves ($N_{good} = 16$), so the second and fifth cuts were used. Oddly enough, χ^2 did not seem to affect N_{good}. This information shows which values for each cut would be used to optimize the search for "good" variables.

IV. Catalog of Selected Objects

A total of 20 candidates were chosen based on their variation and were compared to objects currently catalogued in the SIMBAD astronomical database according to their equatorial coordinates (right ascensions and declinations) [5]. Tables 2 and 3 show lists of candidates that are directly associated with variables that have been previously identified in the SIMBAD astronomical database, as well as some that have coordinates close to those of previously catalogued objects. Using ROTSE1 data, each table shows the object's number, name (according to the SIMBAD database), right ascension and declination, period of variation (T), and range of magnitude variation.

Object #[†]	Object Name[‡]	Right Ascension *(hr. min. sec.)*	Declination *(deg. min. sec.)*	T *(Day)*	Magnitude Range
657	V* HH UMa	11 04 48.11	+35 36 26.60	0.200	11.06 – 10.85
950	2MASS J11372169+4255441	11 37 21.75	+42 55 44.60	0.205	11.67 – 11.37
1127	TYC 3012-1895-1	11 13 45.07	+42 39 51.70	0.320	11.84 – 11.67
1199	V* MT UMa	11 33 34.68	+42 58 29.20	0.400	11.95 – 11.67
1212	V* MU UMa	11 35 36.72	+38 45 57.50	0.500	12.24 – 11.77
1222	V* MQ UMa	11 21 41.02	+43 36 53.00	0.285	11.84 – 11.56
1266	FIRST J111722.9+394253	11 17 19.72	+39 43 03.00	0.450	12.13 – 11.82
1357	V* BS UMa	11 25 41.63	+02 34 48.80	0.175	12.28 – 11.93
1521	V* MP UMa	11 20 37.62	+39 21 00.30	0.070	12.20 – 12.09
1885	2MASS J1116506+3550272	11 16 15.06	+35 50 27.20	0.200	12.85 – 12.46

TABLE 2 *– List of identified variables collected in the April 14, 2000 stare data for camera 'b'. The closest matches in SIMBAD are given.*

Object #[†]	Object Name[‡]	Right Ascension *(hr. min. sec.)*	Declination *(deg. min. sec.)*	T *(Day)*	Magnitude Range
2316	FIRST J113922.2+403640	11 39 28.27	+40 36 32.80	0.255	13.10 – 12.60
2354	-	11 13 40.03	+42 44 13.80	0.210	12.81 – 12.55
2670	-	11 14 15.57	+37 18 25.60	0.050	13.07 – 12.97
2827	SDSS J111055.84+381055.1	11 11 05.45	+38 11 23.50	0.220	13.32 – 13.11
3046	-	11 17 16.02	+38 57 16.90	0.410	13.37 – 13.1
3102	FIRST J112148.9+405909	11 21 48.08	+40 59 38.40	0.210	13.38 – 13.12
3121	GB6 B1117+4411	11 20 09.02	+43 53 49.00	0.310	11.60 – 11.43
3786	FIRST J111740.0+410628	11 17 34.08	+41 06 49.00	0.310	13.70 – 13.20
4751	-	11 03 40.78	+40 26 17.10	0.150	14.10 – 13.50

TABLE 3 *– List of variables collected in the April 14, 2000 stare data that are not closely identified in SIMBAD. The closest objects in SIMBAD are given in Column 2.*

According to the SIMBAD database, the matches with the light sources in the catalog had proven to be either a pulsating variable, eclipsing binary, radio source, quasar, or unidentified. These matches were based on the coordinates of the light source recorded by ROTSE. The "matches" in Table 3 were based on coordinates that were close to those of the ROTSE sources, but no direct matches had been recorded. Table 4 below shows the listing of the variables, their names (if applicable), and the type of variable these sources have been identified in SIMBAD.

Object #[†]	Object Name[‡]	Right Ascension *(hr. min. sec.)*	Declination *(deg. min. sec.)*	Variable Classification[‡]
657	V* HH UMa	11 04 48.11	+35 36 26.60	Pulsating Variable
950	2MASS J11372169+4255441	11 37 21.75	+42 55 44.60	Pulsating Variable
1127	TYC 3012-1895-1	11 13 45.07	+42 39 51.70	Pulsating Variable
1199	V* MT UMa	11 33 34.68	+42 58 29.20	Eclipsing Binary
1212	V* MU UMa	11 35 36.72	+38 45 57.50	Pulsating Variable
1222	V* MQ UMa	11 21 41.02	+43 36 53.00	Eclipsing Binary
1266	FIRST J111722.9+394253	11 17 19.72	+39 43 03.00	Radio Source
1357	V* BS UMa	11 25 41.63	+02 34 48.80	Eclipsing Binary
1459	-	11 13 05.98	+40 21 00.30	-
1521	V* MP UMa	11 20 37.62	+39 21 00.30	Pulsating Variable
1885	2MASS J1116506+3550272	11 16 15.06	+35 50 27.20	Pulsating Variable
2316	FIRST J113922.2+403640	11 39 28.27	+40 36 32.80	Radio Source
2354	-	11 13 40.03	+42 44 13.80	-
2670	-	11 14 15.57	+37 18 25.60	-
2827	SDSS J111055.84+381055.1	11 11 05.45	+38 11 23.50	Quasar
3046	-	11 17 16.02	+38 57 16.90	-
3102	FIRST J112148.9+405909	11 21 48.08	+40 59 38.40	Pulsating Variable
3121	GB6 B1117+4411	11 20 09.02	+43 53 49.00	Radio Source
3786	FIRST J111740.0+410628	11 17 34.08	+41 06 49.00	Radio Source
4571	-	11 03 40.78	+40 26 17.10	-

***TABLE 4** – Total list of variables collected in the April 14, 2000 stare data and their variable "types" according to SIMBAD.*

[†] *According to ROTSE-I 2000 April stare data.*
[‡] *According to SIMBAD astronomical database.*

V. Results

The data contain information regarding the magnitude of the sources' light as a function of intervals of the night recorded as percentages of a day (e.g., 0.30 = 30% of 24 hours, or = 7.2 hours). The light curves shown in Figures 1 – 5 represent relationships of brightness and time, with the levels of magnitude decreasing as the vertical position becomes positive (lower magnitudes correspond to brighter visibility: e.g., magnitude of full moon = -12.6; magnitude of brightest star, Sirius = -1.47). Each light curve grouping below is separated according to the variable type as confirmed by SIMBAD, for those with SIMBAD matches.

These light curves may only show a portion of their periods, T, so an accurate identification for a light source may be difficult to determine without supplemental data. The values for m_{min} and m_{max} are determined by the trough and amplitude of the curve, respectively, and T is determined between the m_{min}'s or the m_{max}'s, depending on the portion of the light curve observed. Although it may be difficult to determine a light source's identity from a small section of its light curve, we can try to infer its nature using the part of the curve that is visible. As the groupings of the light curves in Figures 1-5 show, pulsating variables tend to exhibit an even sinusoidal wave (Figure 1), eclipsing binaries appear to maintain an even m_{max} to which it will abruptly return following an equally rapid decline to the m_{min} (Figure 2), objects in Figure 3 follow a pattern similar to yet more varied than eclipsing binaries, and quasars have a subtle and somewhat random variation (Figure 4). Figure 5 shows a grouping of light curves whose sources have not yet been identified and catalogued in SIMBAD.

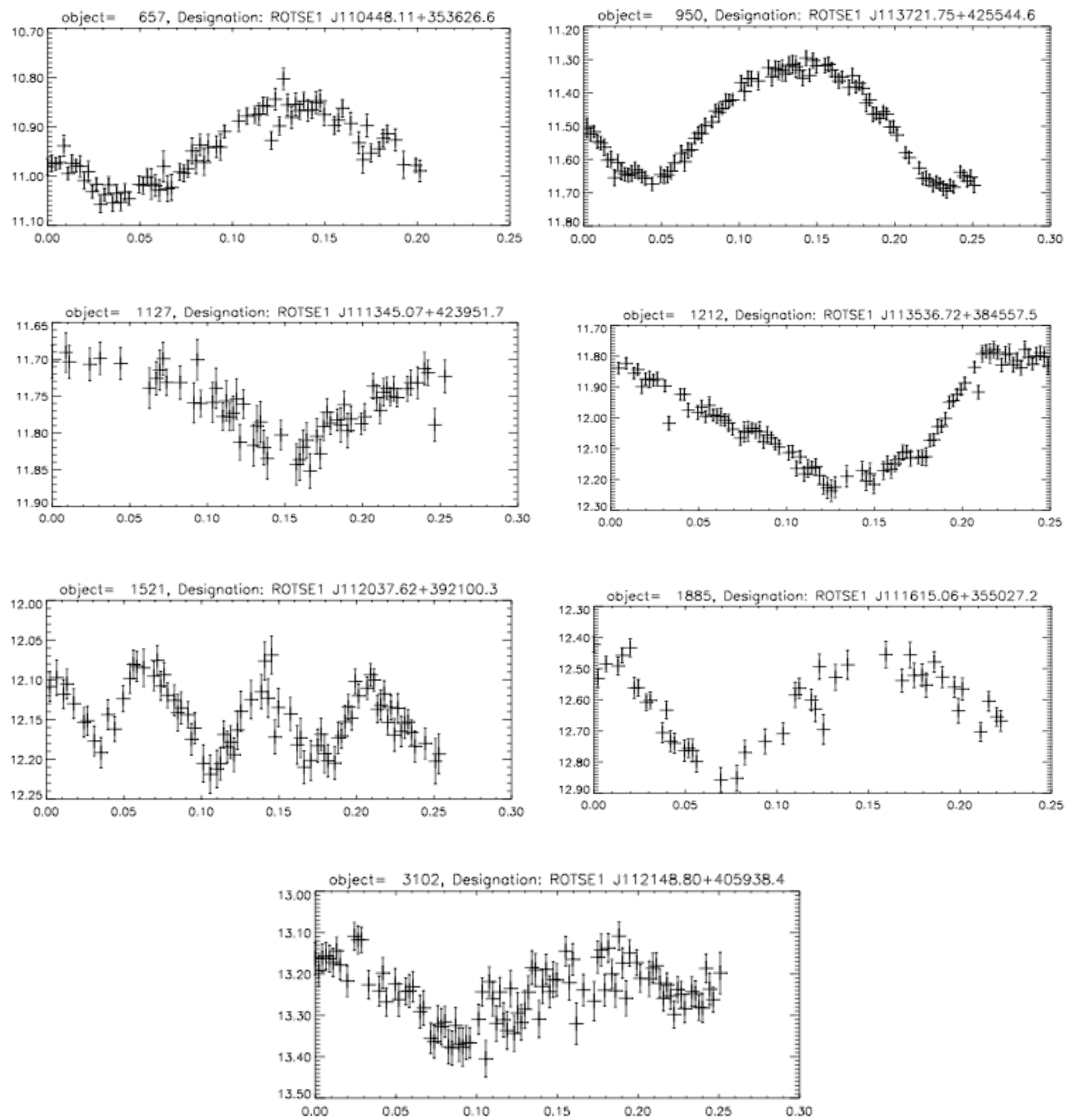

FIG. 1 *- Seven single-night light curves for pulsating variables from the April 14, 2000 stare data. Each of these has previously been identified as variable through the SIMBAD astronomical database. Errors are statistical + systematic.*

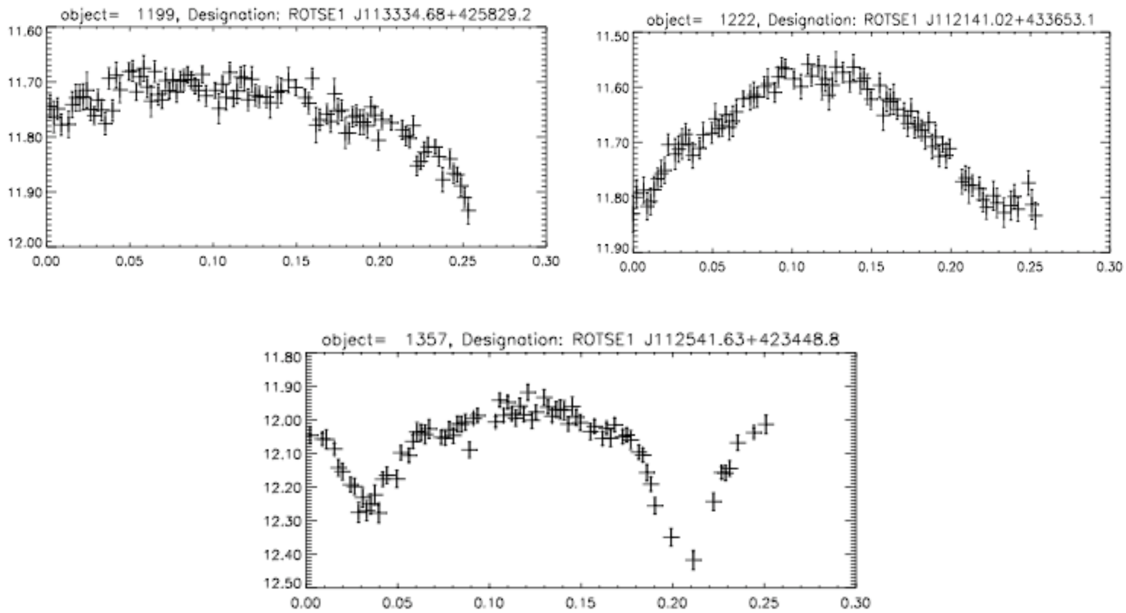

FIG. 2 *- Three single-night light curves for eclipsing binaries from the April 14, 2000 stare data. Each of these has previously been identified as variable through the SIMBAD astronomical database. Errors are statistical + systematic.*

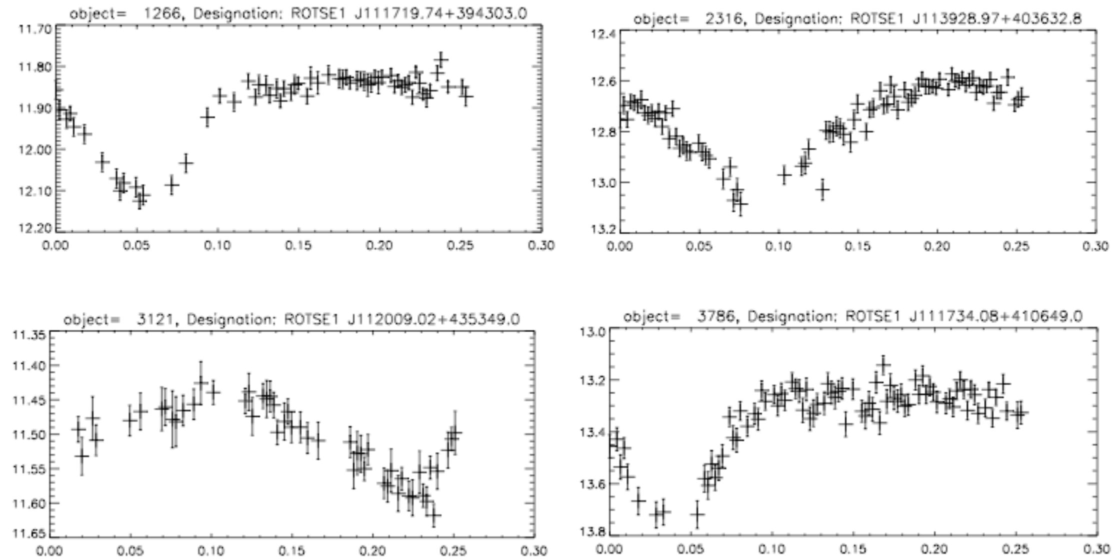

FIG. 3 *- Four single-night light curves for radio sources from the April 14, 2000 stare data. Two of these, objects 1266 and 3121, have previously been identified as radio sources through the SIMBAD astronomical database. Objects 2316 and 3786 have close matches to radio sources in the database. Errors are statistical + systematic.*

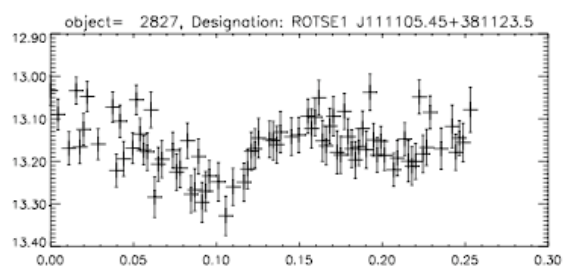

FIG. 4 *- Single-night light curve for a quasar from the April 14, 2000 stare data. This has previously been identified as variable through the SIMBAD astronomical database. Errors are statistical + systematic.*

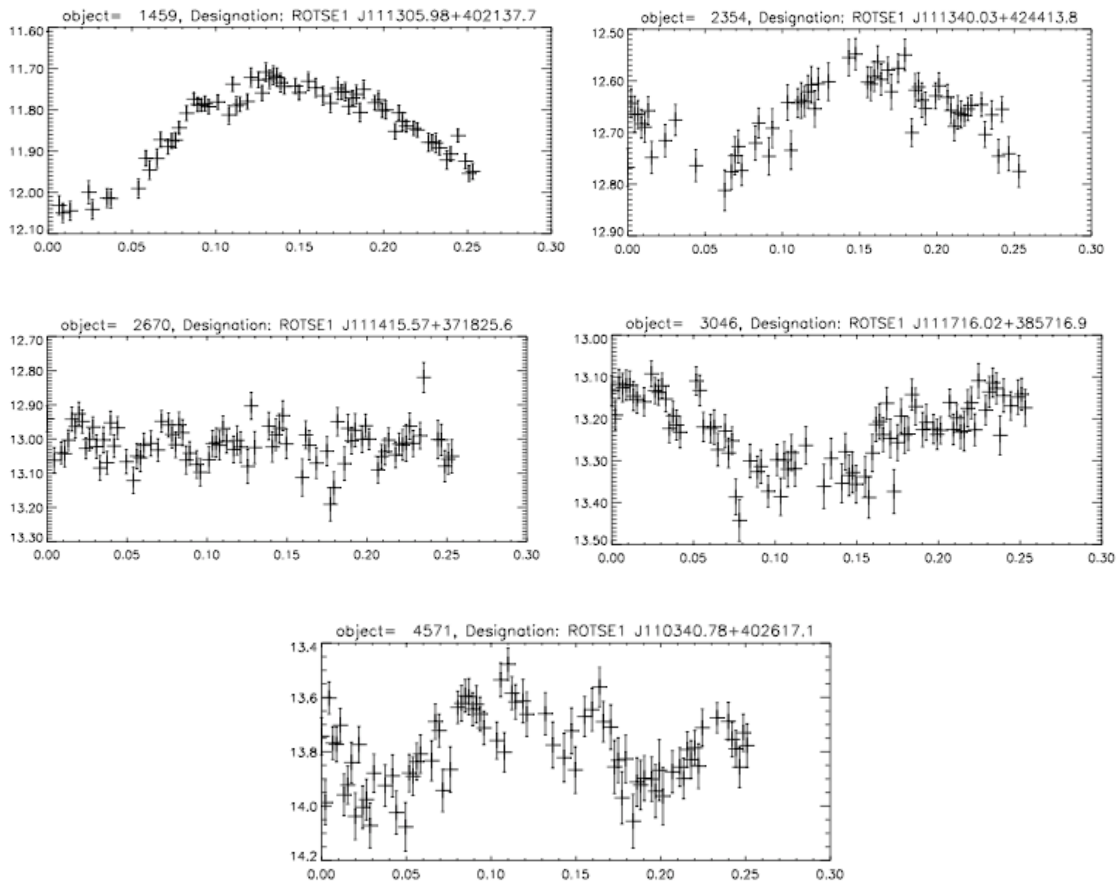

FIG. 5 *- Five single-night light curves for candidate pulsating variables from the April 14, 2000 stare data. None of these have been previously identified. Errors are statistical + systematic.*

The cuts used in this search produced seven pulsating variables, three eclipsing binaries, four potential radio source matches, one quasar, and five newly detected variables. The results yielded a wide variety of variable sources such as δ Scutis with T < 0.1 day (object # 1521), long-period eclipsing binaries (object # 1199, T > 3.0 day), and random radio sources. Of the five new candidates shown, three (object #s 2670, 3046, and 4571) appear to have random variations and could be radio sources, and the other two (object #s 2354 and 1459) may be pulsating and/or eclipsing binaries. It is difficult to determine what these sources may be, since these curves represent only a portion of their variation period. The magnitude levels appear to be similar among the previously identified sources; therefore the magnitudes alone do not allow sufficient information for determining the nature of the unknown sources.

Cepheid variables tend to be fairly young stars (approx. 10^8 years old) with masses several times the solar mass ($M_\odot$), and therefore are highly concentrated within the galactic plane and have low space velocities. [6] Any Cepheid variables would be found near the galactic equator. On the other hand, RR Lyraes are older stars, and therefore can be found within globular clusters at any latitude. The galactic "halo" is a dense, glowing region made of older and dimmer stars, and is semi-spherical in shape as the gravitational forces within the center of the galaxy pull them in. The identified pulsating variables occur well above the galactic equator, and are much closer to the halo region, making them likely candidates for RR Lyrae variables.

The 20 variables found in this search covered a field of view of approximately 65 square degrees (deg.^{2}). The following relation can define the spatial density ρ(s) of stars observable from Earth:

$$\rho(s) \propto \exp\left[\frac{-|z|}{z_0}\right] \quad \textbf{(5)}$$

where s is the orthogonal distance to the source, z is the adjacent distance to the source

($z = s \sin \phi$), ϕ is the source's angle above the galactic plane (declination), and z_0 is the scale height ($z_0 \equiv 97 \pm 7$ parsecs). [7] For this search, the spatial density of variables found may be determined by the number of variables per square degree $\left(\frac{\text{var.}}{\text{deg.}^2}\right)$. The three eclipsing binary variables occurring in the 65 deg.^{2} window have a spatial density of roughly 0.05 $\left(\frac{\text{var.}}{\text{deg.}^2}\right)$, and the seven pulsating variables: $\rho(s) \sim 0.11$ $\left(\frac{\text{var.}}{\text{deg.}^2}\right)$. The other 60% of data consists of radio sources, unknown sources, and a quasar, with spatial densities of 0.06 $\left(\frac{\text{var.}}{\text{deg.}^2}\right)$, 0.08 $\left(\frac{\text{var.}}{\text{deg.}^2}\right)$, and 0.02 $\left(\frac{\text{var.}}{\text{deg.}^2}\right)$, respectively. Equation 5 states that the farther above or below the galactic plane, the fewer stars can be visible. Because the majority of these variables are located so far above the galactic plane, it makes sense that their spatial densities are quite low for this field of view. If we look at more fields, we can determine if Equation 5 holds for each type of variable identified here. With the highest spatial density in this search, pulsating variables appear to be the most common short period variable star in this part of the sky.

VI. Conclusion

The cuts used in this search were few in numbers, but provided adequate results to demonstrate the usefulness of these tools in searching for variable stars. By observing the light curves that were produced using certain cuts, I was able to optimize my selection to find well-measured variables. The 20 light curves selected for this report provided the clearest-varying light curves of all that were generated, and were easily detected among the many images of data. The selected sources were matched with other sources in the

SIMBAD database according to their astronomical coordinates, and this process served to identify the nature of half of the variables. The previously identified sources within the 65 deg.^{2} field of view appear to be seven pulsating variables {ρ(s) ~ 0.11 $\left(\frac{\text{var.}}{\text{deg.}^2}\right)$}, three eclipsing binaries {ρ(s) ~ 0.05 $\left(\frac{\text{var.}}{\text{deg.}^2}\right)$}, four radio sources {ρ(s) ~ 0.06 $\left(\frac{\text{var.}}{\text{deg.}^2}\right)$}, and a quasar {ρ(s) ~ 0.02 $\left(\frac{\text{var.}}{\text{deg.}^2}\right)$}. According to this information, the pulsating variable (RR Lyrae) is the most common type of short period variable star in this field of view. The remaining five sources were unknown, and subsequent night data would provide necessary information to classify these variables. Continuing to research these variables will assist in the understanding of the phenomena that underlie them, and the branch of astrophysics that explains the nature of visibly varying stars.

VII. Nomenclature

D_L	Luminosity Distance, parsec
Δm	Delta Magnitude
m_{max}	Maximum Magnitude
m_{min}	Minimum Magnitude
N_{sat}	Number of Saturated Light Curves
N_{good}	Number of "Good" Light Curves
N_{dim}	Number of Dim Light Curves
s	Distance from Source, Parsec
T	Period of Variation, Day
z	Angular Distance from Source, Parsec
z_0	Scale Height, Parsec
ε	Measurement Error
ε_{max}	Measurement Error on Maximum Magnitude
ε_{min}	Measurement Error on Minimum Magnitude
$\rho(s)$	Spatial Density, $\left(\frac{\text{var.}}{\text{deg.}^2}\right)$
σ_{max}	Maximum Standard Deviation
ϕ	Angle Above Galactic Plane, °
χ^2	Chi-square Distribution

VIII. References

[1] Sterken, C., & Jaschek, C. Light Curves of Variable Stars: A Pictorial Atlas. *Cambridge University Press*, 1996.

[2] Levy, David H. Observing Variable Stars: A Guide for the Beginner. *Cambridge University Press*, 1989.

[3] http://www.rotse.net/

[4] E. Fagg, et al., "General Search for Variable Stars with Rapid Optical Variations: Test Fields", *Journal of Undergraduate Research in Physics*, Vol. 22 (2009).

[5] http://simbad.u-strasbg.fr/simbad/

[6] http://nedwww.ipac.caltech.edu/level5/ESSAYS/Evans/evans.html

[7] William H. Jeffreys, et al. "Model Selection for Cepheid Star Oscillations". http://citeseerx.ist.psu.edu/viewdoc/download?doi=10.1.1.31.8973&rep=rep1&type=pdf